On the contact interaction between two rectangular plates

A. V. Krysko, J. Awrejcewicz, M. V. Zhigalov & V. A. Krysko

Nonlinear Dynamics
An International Journal of Nonlinear Dynamics and Chaos in Engineering Systems

ISSN 0924-090X

Nonlinear Dyn
DOI 10.1007/s11071-016-2858-2

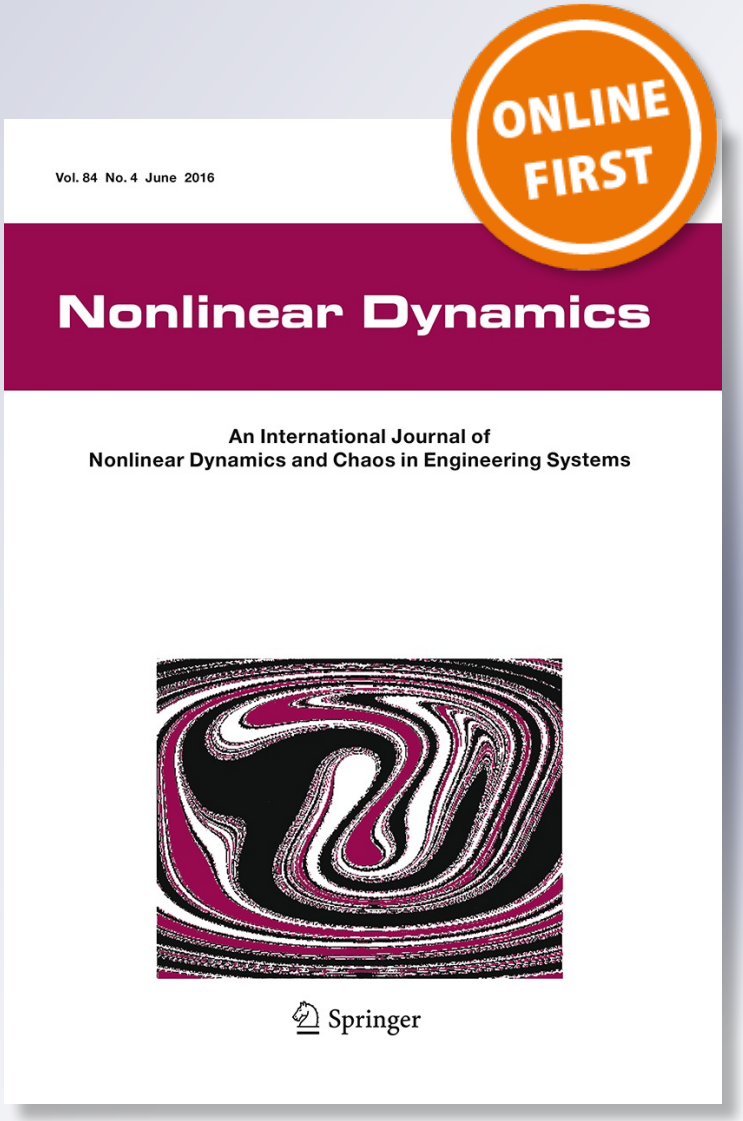

Springer

Nonlinear Dyn
DOI 10.1007/s11071-016-2858-2

ORIGINAL PAPER

On the contact interaction between two rectangular plates

A. V. Krysko · J. Awrejcewicz · M. V. Zhigalov · V. A. Krysko

Received: 2 February 2016 / Accepted: 16 May 2016

Abstract A mathematical model of contact interaction between two plates is presented, considering certain types of nonlinearity of each of the plates. Stress–strain state (SSS) of the interacting structural members is analyzed by the method of variational iterations, and the theorem of convergence of this method is provided. An iterative procedure for solving contact problems is developed and its convergence is also proved. Physical nonlinearity is considered by means of the method of variable parameters of elasticity. The SSS of a two-layer system of rectangular plates, depending on a type of boundary conditions as well as distances between plates, is investigated and supplemented with stress–strain curves $\sigma_i^{(i)}(e_i^{(i)})$for each of the plates.

Keywords Method of variational iterations · Physical nonlinearity · Contact interaction · Method of variable parameters of elasticity

A. V. Krysko
Department of Applied Mathematics and Systems Analysis, Saratov State Technical University, Politehnicheskaya 77, Saratov, Russian Federation 410054
e-mail: anton.krysko@gmail.com

A. V. Krysko
Cybernetic Institute, National Research Tomsk Polytechnic University, Lenin Avenue, 30, Tomsk, Russian Federation 634050

J. Awrejcewicz (✉)
Department of Automation, Biomechanics and Mechatronics, Lodz University of Technology, 1/15 Stefanowski St., 90-924 Lodz, Poland
e-mail: awrejcew@p.lodz.pl

J. Awrejcewicz
Department of Vehicles, Warsaw University of Technology, 84 Narbutta Str., 02-524 Warsaw, Poland

M. V. Zhigalov · V. A. Krysko
Department of Mathematics and Modelling, Saratov State Technical University, Politehnicheskaya 77, Saratov, Russian Federation 410054
e-mail: tak@san.ru

1 Introduction

We begin with a brief historical overview of the sources and state of the art of the papers/books devoted to the problem of impact phenomena and contact interaction of the rigid/flexible structural members. The assessment of strength of elements of plate/shell structures, i.e., damageability of their external layers, requires formulating and solving problems of a unilateral mechanical interaction of thin plates and shells with absolutely rigid bodies (stamps) as well as problems of an interaction of flexible bodies understood further as the 2D objects represented by shells and plates. On the contrary to a bilateral interaction in which contacting bodies form a single object that is obtained, for example, by welding, reaction relations of a one-sided interaction preserve a sign or are equal to zero. On the contrary to the latter approach, in this paper a contact is understood only as a unilateral contact interaction. At a unilateral movement of contact points of the contacting bodies, a condition should be fulfilled that these bodies do not penetrate each other.

Published online: 03 June 2016

The problem of point contact of elastic bodies was formulated and solved for the first time by Hertz [1] in 1882. Later development of technology has put a problem of the contact interaction in a row of actual problems of modern *Solid Mechanics*. Complexity of considered problems has led to a large number of approaches and mathematical methods developed to solve these problems.

Single-layer and multilayer plate models have been studied by Carrera [2] following the earlier introduced Reissner's mixed variational theorem [3,4]. Thin, thick as well as symmetric/asymmetric laminated plates have been analyzed. Matsunaga [5] has applied a two-dimensional, higher-order theory for thick rectangular plates on elastic foundation, and the governing equations have been derived using Hamilton's principle. The employed approximate theories allowed to estimate the natural frequencies and buckling stress of thick plates located on elastic foundations. Kant and Swaminathan [6] have analyzed free vibration of isotropic/orthotropic as well as the multilayer theories. In particular, analytical solutions for the free vibration analysis of laminated composite and sandwich plates have been presented. The natural frequencies and the stress/displacement mode shapes of simply supported, cross-ply laminated and sandwich plates have been evaluated using the propagator matrix method and a semianalytical solution based on a higher-order mixed procedure by Rao et al. [7]. The obtained results have been validated using a 3D elasticity theory.

A novel method to solve free vibration problems for arbitrary shaped orthotropic multilayer plates using the R-functions and Ritz methods have been proposed and applied by Kurpa and Timochenko [8]. Andrews et al. [9] employed theory of bending of beams and plates to study multiply delaminated plate subjected to static, out of plane loading and deforming in cylindrical bending. The authors assumed non-frictional contact along the delamination surfaces and the model has been validated through FEM.

Axisymmetric bending of a package of transversely isotropic two identical plates simply supported has been studied by Zubko and Shopa [10]. The SSS (stress strain state) of the layers has been defined in an analytic way. A similar like analysis has been carried out by Zubko [11], where a thick plate has been divided in an arbitrary number of equally thick layers. Vibration of plates composed of stiff layers and an isotropic viscoelastic core under thermal loads have been investigated by Pradeep and Ganesan [12]. Fiber/angle, ply lay-up and core thickness served as control parameters while studying shifting of modes with temperature. Both authors extended their studies to analyze the thermal buckling and the critical buckling temperature of the multilayer viscoelastic sandwich plates [13].

Loredo and Castel [14] have investigated vibrations of a package of inhomogeneous anisotropic multilayered plates taking into account transverse shear variation through the plate thickness using the warping functions. The developed by them model is suitable for both static and dynamics analysis, and its efficiency has been proven. Altukhov et al. [15] have studied vibrations of a two-layer plate of arbitrary thickness with rigidly fixed plane faces and sliding contact of layers. The problem has been reduced to the 2D boundary value problem, and influence of the mechanical and geometric parameters on the phase/group velocities, as well as the problem regarding cutoff frequencies have been analyzed. Pull-in instability of nanoswitches made of two parallel plates subjected to electrostatic force has been investigated in reference [16]. The nanoplates with opposite charges have been modeled based molecular dynamics technique. Influence of different initial gaps between nanoplates, and geometric/physical parameters, have been taken into account while evaluating pull-in voltages.

Malekzadeh et al. [17] have investigated influence of some geometrical, physical and material parameters on free vibration response of the composite plates embedded with shape memory alloy wires. Transverse shear and rotary inertia effects have been taken into account. Akoussan et al. [18] have analyzed vibrations of orthotropic multilayer sandwich structures with viscoelastic core. The finite element-based numerical study aimed on variation of the damping properties of the structures versus the faces material fibers orientation. Pietrzakowski [19] has studied random vibrations of an actively damped laminated plate with functionally graded piezoelectric actuator layers. The random input has been assumed as a Gaussian stationary and ergodic process, whereas the actuators have been arrays of piezofibers composite sublayers. The power spectral density, autocorrelation function, and variances have been numerically estimated to recognize the influence of the applied random excitation on the characteristics of the stochastic field of active plate deflection.

The carried out brief review of the state of the art of the composite/laminate plates as well as multilayer/two-layer packages of plate shows importance of the novel theoretical approaches for modeling and analysis of the mentioned structural members. Problems of the contact interaction between thin shells/plates are especially difficult as, while solving them, it is necessary to define simultaneously both the SSS and zones of contact of two or more contacting thin-walled objects. Generally, these structural members may have also various shape and design-type nonlinearity.

It should be emphasized that this problem has a long history also in Eastern oriented literature. The simplest linear problem definition is the one for cylindrical shells of varying length, mounted with a tight fit. Without considering compression, i.e., when the solution concerns transverse forces concentrated on the contact zone border, the problem has been studied in references [20–22], and the derived differential/integral equations have been solved. Compression was introduced to the Winkler model in the work [23], and to a model of an elastic cylinder and a layer – in references [24,25]. In the two latter works contact pressure becomes infinite on borders of contact zones. This problem was investigated with the use of the Timoshenko theory in [26].

An interaction of two spherical shells has been analyzed with the help of the Kirchhoff–Love theory in [27]. It was found that the contact reaction is in fact the concentrated force distributed along the circumference. The solution based on Timoshenko theory was given in [28]. The contact pressure at the boundary of the contact zone was equal to zero, although it was to have taken a finite nonzero value.

The problem of contact between two rectangular plates was solved by the variational differential method in paper [29]. The above-mentioned studies are based on the linear shell theory. Geometrically nonlinear shell theory is applied in work [30] to study contact between the layers of goffer membranes by means of the finite element method. Contact conditions are physically represented by special nonlinear elements between the nodes of the contacting layers.

Mechanical behavior of laminated shells with a non-ideal interface of layers constitutes a separate class of contact problems. To create a theory of such thin shells and methods of their calculation, discrete approach is usually used. Complete system of relations of the chosen shell theory is recorded for each of the layers and then closed by kinematic and static layer interference conditions (both equalities and inequalities). The order of a system of differential equations obtained in this way is N times (N—number of layers) the order of the layer.

If normal displacement and tension of the layer contact surfaces coincide, and shear stress is equal to zero, we come to the problem for a shell with layers that slip without friction. Thus, contact zones are known, which significantly simplifies the problem. In this manner, static problems of layered cylindrical [31] and spherical [32] shells have been solved. The method of consecutive approximations, based on the "*principle of sequential continuity*", according to which boundary problems for the layers are solved independently at each iteration, was applied in references [33,34] to study layered cylinders and cylindrical shells. Problems of the contact interaction between thin plates and shells are difficult since, while solving them, it is necessary to simultaneously define the SSS and contact zones of two and more plates and shells. The considered plates and shells are generally of various shapes. Contact of two circular plates separated with a gap, in the case when one of them is loaded, was studied by Artyukhin and Karasev [35] with the use of the Kirchhoff theory. At the boundary of the contact zone, the concentrated force and momentum were found. Applying the Timoshenko theory to solve axisymmetric problems allows to obtain the finite value of the contact pressure at the boundary [36]. Discrete approach using Timoshenko theory for layered plates is implemented in [37] by means of the matrix method proposed by the authors. This method yields a system of integral equations of the contact pressure in a priori unknown zones. It also takes into account the possibility of ruptures of the interface layers.

However, our approach presented in this paper goes beyond the literature reports and opens a novel challenging research topic matching bifurcation/chaotic vibrations with non-smooth contact dynamics exhibited by 2D continuous systems of infinite dimension. Our research is main motivated by two reasons. First, laminated composite plates and multilayer plates are widely applied in numerous industrial branches, including civil engineering, ship building, aeronautics, aerospace, as well as in the developing fields of modern technology. In the latter case in the used navigation devices and electronics techniques, the multilayer flat micromechanical accelerometers are applied. They are usually modeled by packages of plates and beam, where

the plate(s) are reinforced by a set of plates/beams with constraints. Appearance of even small constraints/gaps between the structural members (plates–beams, plates–plates) exhibits a various interesting and sometimes unexpected nonlinear behavior [38,39].

On the other hand, an important role in applications play micromechanical gyroscopes including fiber optic, spherical resonator gyroscopes as well as Coriolis vibratory gyroscopes [40–43]. The industrial needs attracted recently observed interest in modeling and a study of gyroscopes and other nano-electrostatically activated cantilever and fixed–fixed beams have been studied taking into account the beams length, width and thickness as well as the gap between the beams and ground plate [44].

A doubly clamped suspended beams coupled to one adjacent stationary electrode has been analyzed both theoretically and experimentally by Buks and Roukes [45]. Three continuous mass sensors composed of parallel interdigital comb finger banks and two sets of non-interdigitated comb fingers on each side supplemented by four folder beams, served as an auto-parametric amplificatory, have been modeled and studied by Zhang et al. [46].

The earlier described design of gyroscopes and other micro-mechanical devices can be directly modeled by the structural members like plates and beams within gaps between them. In this case, however, as the existing literature review shows, only reduced ordered models are derived mainly, and hence the obtained results may be not valid in the whole working regimes of those devices (for example, in this case the multimode interactions are neglected). In the case of the earlier described state of the art of laminated composite plates and packages of multilayer plates the previously welded or glued layers may lose their permanent contact due to the mentioned object long working regimes, and hence the problem of contact/non-contact between structural members while their vibrations plays a crucial role.

In addition, in spite of the technological inspired motivation of our research, there is a challenging interest in modeling and analysis of the mentioned objects from a theoretical point of view since we do not know papers dealing with this research topic.

The analysis of a current state of solving contact interaction problems shows that the case of two rectangular plates has not been considered taking into account nonlinear relationship between stress and strain. The present paper is devoted to this subject, and it is organized in the following way. The problem is defined and theoretically founded in Sect. 2. The applied iterative algorithms are validated in Sect. 3, whereas Sect. 4 presents numerical results regarding contact interaction of two squared plates. The paper is finished by giving concluding remarks in Sect. 5.

2 Problem statement

We consider the problem of a unilateral mechanical interaction between two rectangular plates (Fig. 1). The plates are assumed to be thin and their stress–strain state (SSS) is described with the classical Kirchhoff theory supplemented with physical nonlinearity according to the theory of small elasto-plastic deformations. We will assume that the contact pressure (normal to surface stress) is much less than normal stresses occurred in the cross sections of the plates. Moreover, it is assumed that the plates slip freely in contact zones. (In other words, friction phenomena are not taken into account here).

The choice of the classical plate theory is motivated by that fact that the SSS and the contact pressure distribution of the effect of transverse shear deformation is much weaker than transverse compression in the contact zone [47]. Consideration of the latter factor is one of the foundations of the proposed approach. We construct an initial system of differential equations for two contacting plates in the following form [48]:

$$\begin{cases} A_1 w_1(x, y) = q_1(x, y) - q_k \psi, \\ A_2 w_2(x, y) = q_2(x, y) + q_k \psi, \end{cases} \tag{1}$$

where $w_i(x, y)$—vector function, $q_i(x, y)$—vector of external load, i—number of a plate, counted in the positive direction of the normal, Ω_1, Ω_2—areas of the plates, $\partial\Omega_i (i = 1, 2)$ - boundary regions.

The operator $A_i (i = 1, 2)$ takes the following form for physically linear problems:

$$A_i w_i\,(x, y) = D\frac{\partial^2}{\partial x^2}\left(\frac{\partial^2 w_i}{\partial x^2} + \frac{\partial^2 w_i}{\partial y^2}\right) + \frac{\partial^2}{\partial y^2}\left(\frac{\partial^2 w_i}{\partial x^2} + \frac{\partial^2 w_i}{\partial y^2}\right), \tag{2}$$

where $D = \frac{E_i h^3}{12(1-\nu_i^2)}$ - cylindrical stiffness; E_i—Young's modulus, ν_i—Poisson ratio.

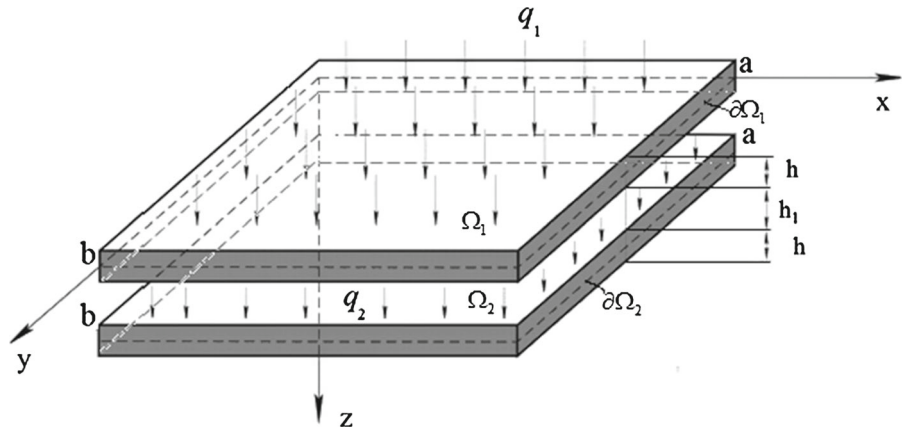

Fig. 1 Two interacting plates of thickness h with the normal loads $q_i(x, y)$ and the gap h_1

On the other hand, the operator A_i $(i = 1, 2)$ takes the following form for physically nonlinear problems:

$$A_i w_i(x, y) = \frac{\partial^2}{\partial x^2}\left(B_{11,i}\frac{\partial^2 w_i}{\partial x^2} + B_{10,i}\frac{\partial^2 w_i}{\partial y^2}\right) + \frac{\partial^2}{\partial y^2}\left(B_{10,i}\frac{\partial^2 w_i}{\partial x^2} + B_{11,i}\frac{\partial^2 w_i}{\partial y^2}\right) + 2\frac{\partial^2}{\partial x \partial y}\left(\left(B_{11,i} - B_{10,i}\right)\frac{\partial^2 w_i}{\partial x \partial y}\right), \tag{3}$$

where

$$B_{mn,i} = \frac{1}{2}\left[\frac{E_{11,i}}{E_{01,i}} + (-1)^{n+1}\frac{E_{10,i}}{E_{00,i}} - E_{21,i} + (-1)^n E_{20,i}\right],$$

$$E_{mn,i} = \int_{a_i(x,y)}^{b_i(x,y)} \frac{E_i z^m}{1+(-1)^n \nu_i}\,\mathrm{d}z, \quad (n=0, 1; m=i=1, 2).$$

Here $z = a_i(x, y), z = b_i(x, y), (x, y) \in \Omega_i$ are equations of external surfaces of the plates, allowing to consider the thickness variability of each of the plates in further performed computations; $E_i(x, y, z, e_i^{(i)})$, $\nu_i(x, y, z, e_i^{(i)})$ stand for the variable elasticity modulus and Poisson's ratio of the plates, $e_i^{(i)}$ is the intensity of deformation (i) of the plate $(i = 1, 2)$.

Two types of boundary conditions are taken into account:

(a) simple support:

$$w_i\Big|_{\partial\Omega} = \frac{\partial^2 w_i}{\partial n^2}\Big|_{\partial\Omega} = 0, \quad i = 1, 2; \tag{4}$$

(b) clamping:

$$w_i\Big|_{\partial\Omega} = \frac{\partial w_i}{\partial n}\Big|_{\partial\Omega} = 0, \quad i = 1, 2. \tag{5}$$

Contact pressure in the contact zone is proportional to transverse compression $w_1 - h_1 - w_2$, and hence

$$q_k(x, y) = k\frac{E}{h}(w_1 - h_1 - w_2). \tag{6}$$

In addition, the function ψ can be written as follows

$$\psi = [1 + sign(w_1 - h_1 - w_2)]/2, \tag{7}$$

where h_1 stand for the gap between plates, and k denotes stiffness coefficient of transverse compression of plates.

Equation (6) is valid for the case of contact of plates of identical thickness h and identical values of k. For contact problems within the Kirchhoff theory of plates, Winkler relationship between compression and contact pressure is applied [49].

If the initial arrangement of plates (gap function h_1) and the load are such that during deformation the plates do not come into contact, then $\psi \equiv 0$ and the system of Eq. (1) is separated into two independent systems. Otherwise, (1) creates a coupled system. After substituting (6) to (1) one gets:

$$\begin{cases} A_1 w_1(x, y) = q_1(x, y) - k\frac{E}{h}(w_1 - h_1 - w_2)\psi, \\ A_2 w_2(x, y) = q_2(x, y) + k\frac{E}{h}(w_1 - h_1 - w_2)\psi. \end{cases} \tag{8}$$

The system (8) of the eighth order should be considered together with boundary conditions 4, 5. It should be emphasized that it constitutes both structurally and physically nonlinear problem of the eighth order [49].

In order to solve a structurally nonlinear problem (8), one can construct an iterative process that allows to consistently solve only one of the system equations (8) at each step of loading. Such an approach makes it possible to reduce twice the order of the system of equations for a two-layer problem. In general, the order can be reduced n times for n layers. The iterative procedure can be written in the following form:

$$\begin{cases} A_1(w_1^{(n)}) + k\frac{E}{h}\psi_{(n-1)}w_1^{(n)} \\ \quad = q_1(x,y) + k\frac{E}{h}\left(h_1 + w_2^{(n-1)}\right)\psi_{(n-1)}, \\ A_2(w_2^{(n)}) + k\frac{E}{h}\psi_{(n-1)}w_2^{(n)} \\ \quad = q_2(x,y) + k\frac{E}{h}\left(w_1^{(n-1)} - h_1\right)\psi_{(n-1)}. \end{cases} \tag{9}$$

It is necessary to supplement the system (9) with the corresponding boundary conditions 4 or 5 for the i-th plate.

The algorithm for solving (9) consists of the following steps: The procedure of the variational iteration method (VIM) is constructed at the fixed contact zone to obtain a solution to the given accuracy and supplemented with the method of variable elasticity parameters followed by the specification of the contact zone by means of the simple iteration method. The procedure is then repeated, i.e., there are three iterative procedures, nested one inside the other.

As an example, let us consider an iterational procedure of the contact pressure estimation in the case of two-layer rectangular isotropic plate. In this case, the operators A_i in Eq. (1) take the form (2), whereas PDEs (1) are cast to the following form

$$\begin{aligned} D\Delta^2 w_1 &= q - c\,(w_1 - w_2)\,\psi, \\ D\Delta^2 w_2 &= q + c\,(w_1 - w_2)\,\psi, \end{aligned} \tag{10}$$

where: $\psi = [1 + sign(w_1 - w_2)/2]$.

Simple reformulation of Eq. (10) yields

$$\begin{aligned} D\Delta^2(w_1 + w_2) &= 2q, \\ D\Delta^2(w_1 - w_2) + 2c\,(w_1 - w_2)\,\psi &= 0, \end{aligned} \tag{11}$$

where $c = k\frac{E}{h}$.

If we take $\psi = 1$, both of Eq. (11) are decoupled. The first one presents a solution regarding summed stiffness of the two plates, whereas the second describes the contact pressure between them. The iterations are only needed to improve the function ψ. It has been shown through numerous numerical experiments that the presented algorithm yields fast convergence, whereas the introduced parameter c does not influence the convergence.

Formally, the VIM scheme consists of the following steps. At first, let us find the solution to the equation:

$$Aw(x,y) = q(x,y); \quad x, y \in \Omega(x,y), \tag{12}$$

where: A—an operator defined on a set $D(A)$ of the Hilbert space $L_2(\Omega)$; $q(x,y)$—given function of two variables x and y; $w(x,y)$—the unknown function of the same variables; $\Omega(x,y)$—domain of variables x and y.

If $\Omega(x,y) = X \times Y$ (X—a limited set of variables x, Y—bounded set of y), then the solution to (10) takes the form:

$$w_N(x,y) = \sum_{i=1}^{N} u_i(x)v_i(y), \tag{13}$$

where functions $u_i(x)$ and $v_i(y)$ are derived from the system of equations

$$\begin{aligned} &\int_X (Aw_N - q)\,u_1(x)\,\mathrm{d}x = 0, \quad \int_Y (Aw_N - q)\,v_1(y)\,\mathrm{d}y = 0, \\ &\cdots \qquad\qquad\qquad\qquad \cdots \\ &\int_X (Aw_N - q)\,u_N(x)\,\mathrm{d}x = 0, \quad \int_Y (Aw_N - q)\,v_N(y)\,\mathrm{d}y = 0, \end{aligned} \tag{14}$$

in the following manner: A system of N functions is set for one of the variables, e.g., $u_1^0(x), u_2^0(x), \ldots, u_N^0(x)$, and from the first N equations of the system (14), the system of N functions $v_1^1(x), v_2^1(x), \ldots, v_N^1(x)$ is defined. Then, the obtained functions create a new system of functions for the variable $x - u_1^2(x), u_2^2(x), \ldots, u_N^2(x)$, from which new functions are defined for the variable $y - v_1^3(x), v_2^3(x), \ldots, v_N^3(x)$, etc.

The following theorems have been proved being a theoretical justification of VIM convergence for problems of the plate theory [49].

Theorem 1 *If A is a positive definite operator of a domain $D(A) \subset H_A$, then the sequence of elements $\alpha_k = \left\|w_1^k(x,y) - w_0\right\|_{H_A}$ monotonically decreases, i.e., for all i and j such that $i \geq j$, we have*

$$\left\|w_1^i - w_0\right\|_{H_T} \leq \left\|w_1^j - w_0\right\|_{H_T}. \tag{15}$$

Theorem 2 *Let each of the elements of the space* $\dot{W}_2^m(X \times Y)$ *have the form*

$$\theta_i(x, y) = \varphi_i(x)\,\psi_i(y), \tag{16}$$

where $\{\varphi_i(x)\}$ *is a basis system in* $\dot{W}_2^m(X)$ *space and* $\{\psi_i(y)\}$*—in a* $\dot{W}_2^m(Y)$ *space. For any N-th approximation of the VIM, constituent elements of the basis system* $\{\theta_i(x, y)\}$ *are taken as primary functions. In this manner, for sufficiently large N, the VIM results in an approximation* ω_N*, and in the space* $\dot{W}_2^m(X \times Y)$ *a sequence* $\{w_N\}$ *converges to the exact solution* ω_0*, regardless of the number of steps k that can be done for each N-th approximation, i.e.,* $\left\| w_N^k - w_0 \right\|_{W_2^{m0}} \to 0$, $N \to \infty$.

Ordinary differential equations (ODEs) obtained with the use of variational iteration method at each step of the iterative procedure can be solved in different ways. For example, the finite difference method (FDM) can be used and followed by a solution to the resulting system of algebraic equations with the use of the Gauss method.

The variational iteration method allows not to construct the system of approximating functions, on the contrary to the Bubnov–Galerkin and Ritz methods. At the beginning, a system of functions is arbitrarily chosen (it must meet some well-known conditions of smoothness). Then, it is specified during computations with the VIM, based on the solutions of the original system of differential equations of the plate theory. Thus, the VIM automatically builds the approximating functions both at the boundaries and within the region of interest. The disadvantage of the method is that the temporarily unknown function of two variables is represented as a product of two functions, and each of these functions depends on a single argument, as in the Fourier method. This leads to the need to solve two ordinary differential equations instead of one. In fact, the variational iteration method is a generalization of a Fourier method.

To illustrate the above-mentioned idea, we present the solution to the biharmonic Eq. (2) with the boundary conditions 4 and 5 for the domain Ω=$(0, a) \times (0, b)$, where $\partial\Omega$ stands for the boundary of Ω. Both the differential equation and the boundary conditions are transformed into a dimensionless form using following relations: $x = \bar{x}a$, $y = \bar{y}b$, $w = \bar{w}h$, $\lambda = \frac{a}{b} = 1$, $\bar{q}(x, y) = \frac{q(x,y)}{12(1-\nu^2)}\,\frac{a^4}{Eh^4}$, $\nu = 0.3$.

Table 1 Deflection of the plate center estimated by VIM versus exact solution

1	Name of the method	$w(0, 5; 0, 5)$	
		Boundary conditions 4	Boundary conditions 5
1	Variational iteration method (VIM)	0.2030	0.06483
2	Exact solution	0.2028	0.0631

Table 1 presents deflections at the center $w(0, 5; 0, 5)$ of a one-layer plate, implied by constant load $q(x, y) = 50$ action.

Two types of the boundary functions $w_1(x)$, $w_2(y)$ satisfying boundary conditions 4 and 5 were taken in the form: $w_1(x) = 1$; $w_2(y) = 1$ as an initial approximation. The VIM procedure has ended at the fourth iteration. In this case, one can observe an almost complete agreement of the exact solution with the boundary condition 4: The difference was equal to 0.1 %, while for the boundary condition 5 the difference was equal to 0.6 %.

The method of variable elasticity parameters [50] is used for the solution to physically nonlinear problems, assuming that $E_i(x, y, z, e_i^{(i)})$, $\nu_i(x, y, z, e_i^{(i)})$ are not constant, but depend on the strain state at the point determined by the following formulas [50]:

$$E_i = \frac{9K_{1i}G_i}{3K_{1i} + G_i}, \quad \nu_i = \frac{1}{2}\frac{3K_{1i} - 2G_i}{3K_{1i} + G_i}. \tag{17}$$

Here we assume that the volume deformation $K_{1i} = const$. In the deformation theory of plasticity shear modulus is determined by the following relation:

$$G_i = \frac{1}{3}\frac{\sigma_i^{(i)}(e_i^{(i)})}{e_i^{(i)}}, \tag{18}$$

where $\sigma_i^{(i)}$, $e_i^{(i)}$ denotes intensity of stresses and strains $(i = 1, 2)$ of the plate, respectively, and

$$e_k^{(i)} = \frac{\sqrt{2}}{3}\left[\left(e_{xx}^{(i)} - e_{yy}^{(i)}\right)^2 + \left(e_{yy}^{(i)} - e_{zz}^{(i)}\right)^2 + \left(e_{xx}^{(i)} - e_{zz}^{(i)}\right)^2 + 1.5\left(e_{xy}^{i}\right)^2\right]^{1/2},$$

$$e_{xx}^{(i)} = -z\frac{\partial^2 w_i}{\partial x^2}, \quad e_{yy}^{(i)} = -z\frac{\partial^2 w_i}{\partial y^2}, \quad e_{xy}^{(i)} = -2z\frac{\partial^2 w_i}{\partial x \partial y}. \tag{19}$$

In formula (19), $e_{zz}^{(i)}$ is derived from the condition of plane stress ($\sigma_{zz} = 0$), i.e.:

$$e_{zz}^{(i)} = -\frac{\nu_i}{1-\nu_i}\left(e_{xx}^{(i)} + e_{yy}^{(i)}\right). \tag{20}$$

In the next section we prove a theorem of the convergence of the iterative procedure (9).

3 The proof of convergence of iterative algorithms of the solution to the studied contact problems

Let R^2 be an Euclidean plane with a Cartesian basis, and $\Omega_i \in R^2$—the area of the plate including the boundaries $\partial\Omega_i$ (i = 1, 2), $\bar{\Omega}_i = \Omega_i \cup \partial\Omega_i$ $(x, y) \in \Omega_i$, Ω^*—subdomain of Ω_i, $\forall i$, $\Omega^* \subseteq \Omega_i$, n_i—normal external to $\partial\Omega_i$.

Let us consider a spatial plate system consisting of two plates being in contact. The system is described with the Kirchhoff's hypotheses, and the following governing equations hold:

$$\begin{cases} A_1(w_1(x,y)) + k\frac{E}{h}w_1\psi(x,y) \\ \quad = q_1 + k\frac{E}{h}(w_2 + h_1)\psi(x,y), \\ A_2(w_2(x,y)) + k\frac{E}{h}w_2\psi(x,y) \\ \quad = q_2(1-\psi(x,y)) + k\frac{E}{h}(w_1 - h_1)\psi(x,y), \end{cases} \tag{21}$$

with the boundary conditions 5. The function defining contact zones $\Omega^*$of plates has the following form:

$$\psi(x,y) = \begin{cases} 1, & (x,y) \in \Omega*, \\ 0, & (x,y) \notin \Omega*, \end{cases}$$

whereas $q_1(x,y), q_2(x,y)$ are functions of the external loads acting on the first and second plate, respectively; operators $A_i(w_i)$ have the form (3), which for the elastic problem takes the form (2); $||\cdot||_A$—norm in a normed vector space A; $(\cdot,\cdot)_B$—scalar product in Hilbert space L_2. Identification of functional spaces corresponds to that described in monograph [51].

In order to solve the problem (21), (5), the following iterative algorithm is used:

$$\begin{aligned} &A_1(w_1^{(n+1)}(x,y)) + k\frac{E}{h}w_1^{(n+1)}\psi(x,y) \\ &\quad = q_1 + k\frac{E}{h}(w_2^{(n)} + h_1)\psi(x,y), \\ &A_2(w_2^{(n+1)}(x,y)) + k\frac{E}{h}w_2^{(n)}\psi(x,y) \\ &\quad = q_2(1-\psi(x,y)) + k\frac{E}{h}(w_1^{(n)} - h_1)\psi(x,y), \end{aligned} \tag{22}$$

$$\begin{aligned} &w_1^{(n+1)}\Big|_{\partial\Omega_1} = \frac{\partial w_1^{(n+1)}}{\partial n_1}\Big|_{\partial\Omega_1} \\ &\quad = 0,\ w_2^{(n+1)}\Big|_{\partial\Omega_2} = \frac{\partial w_2^{(n+1)}}{\partial n_2}\Big|_{\partial\Omega_2} = 0. \end{aligned} \tag{23}$$

Theorem 3 *Let Ω_i, (i = 1, 2) be a restricted area, whose boundaries $\partial\Omega_i$ satisfy the Sobolev embedding theorem [51], Ω^*—measurable area, $q_i(x,y) \subseteq L_2(\Omega_i)$ and, apart from that, physical constants $c_i > 0$, $D_i > 0$ are such that*

$$\begin{aligned} &D_1 \|\Delta(w_i)\|^2_{L_2(\Omega^*)} \\ &\le \left(B_{11,i}\frac{\partial^2 w_i}{\partial x^2} + B_{10,i}\frac{\partial^2 w_i}{\partial y^2}, \frac{\partial^2 w_i}{\partial x^2}\right)_{L_2(\Omega_2)} \\ &\quad + \left(B_{10,i}\frac{\partial^2 w_i}{\partial x^2} + B_{11,i}\frac{\partial^2 w_i}{\partial y^2}, \frac{\partial^2 w_i}{\partial y^2}\right)_{L_2(\Omega_2)} \\ &\quad + \left[\left(B_{11,i} + B_{10,i}\right)\frac{\partial^2 w_i}{\partial x \partial y}, \frac{\partial^2 w_i}{\partial x \partial y}\right]_{L_2(\Omega_2)} \\ &\le c_i \|\Delta(w_i)\|^2_{L_2(\Omega_i)}. \end{aligned}$$

Then:

(1) $\forall n, w_i^{(n)} \in W_2^4(\Omega_i) \bigcap \dot{W}_2^2(\Omega_i)$, i = 1,2;

(2) There exist functions $w_i^*(x,y) \in \dot{W}_2^2(\Omega_i)$, $i = 1, 2$, being a solution to (20), (3), and at the same time $\lim\limits_{n\to\infty}\left\|w_i^{(n)} - w_i^*\right\|_{W_2^2(\Omega_i)} = 0$.

Proof We describe main stages of the proof. Implementation of the first conclusion of the theorem is provided under the condition that the initial approximations $w_i^0 \in L_2(\Omega_i)$, $i = 1, 2$, follow from the theory of resolvability of the elliptic Eq. [51].

The second conclusion of the theorem proves the existence of a generalized solution to (20), (3) in the space $\dot{W}_2^2(\Omega_1) \times \dot{W}_2^2(\Omega_2)$ and strong convergence of the sequence of approximate solutions $\{w_i^{(n)}\}$ to the exact solution w_i^* in the norm $\dot{W}_2^2(\Omega_i)$, $i = 1, 2$. To justify the second conclusion of the theorem, the following operations are implemented:

(1) subtraction of corresponding equations defining functions $w_i^{(n)}(i = 1, 2)$ from each of the equations of the system (22);

(2) multiplication of the first equation of the resulting system by $(w_1^{(n+1)} - w_1^{(n)})$, and of the second equation by $(w_2^{(n+1)} - w_2^{(n)})$;
(3) integration of the first of the obtained equations over the area Ω_1, and the second—over Ω_2. As a result, after using Green formula, we get:

$$\begin{aligned}
&\left(B_{10,1}\frac{\partial^2\left(w_1^{(n+1)}-w_1^{(n)}\right)}{\partial x^2}\right.\\
&\left.+B_{10,1}\frac{\partial^2\left(w_1^{(n+1)}-w_1^{(n)}\right)}{\partial y^2},\frac{\partial^2\left(w_1^{(n+1)}-w_1^{(n)}\right)}{\partial x^2}\right)_{L_2(\Omega_2)}\\
&+\left(B_{10,1}\frac{\partial^2\left(w_1^{(n+1)}-w_1^{(n)}\right)}{\partial x^2}\right.\\
&\left.+B_{11,1}\frac{\partial^2\left(w_1^{(n+1)}-w_1^{(n)}\right)}{\partial y^2},\frac{\partial^2\left(w_1^{(n+1)}-w_1^{(n)}\right)}{\partial x^2}\right)_{L_2(\Omega_2)}\\
&+\left(\left[B_{11,1}-B_{10,1}\right]\frac{\partial^2\left(w_1^{(n+1)}-w_1^{(n)}\right)}{\partial x\partial y},\frac{\partial^2\left(w_1^{(n+1)}-w_1^{(n)}\right)}{\partial x\partial y}\right)_{L_2(\Omega_1)}\\
&+\frac{kE}{h}\left(\psi(x,y)\left(w_2^{(n)}-w_2^{(n-1)}\right),\right.\\
&\left.\frac{kE}{h}\left(\psi(x,y)\left(w_1^{(n+1)}-w_1^{(n)}\right),\left(w_1^{(n+1)}-w_1^{(n)}\right)\right)_{L_2(\Omega_1)}\right.\\
&=\left.\frac{kE}{h}\left(\psi(x,y)\left(w_2^{(n)}-w_2^{(n-1)}\right),\left(w_1^{(n+1)}-w_1^{(n)}\right)\right)_{L_2(\Omega_1)},\right. \quad (24)\\
&\left(B_{11,2}\frac{\partial^2\left(w_2^{(n+1)}-w_2^{(n)}\right)}{\partial x^2}\right.\\
&\left.+B_{10,2}\frac{\partial^2\left(w_2^{(n+1)}-w_2^{(n)}\right)}{\partial y^2},\frac{\partial^2\left(w_1^{(n+1)}-w_1^{(n)}\right)}{\partial x^2}\right)_{L_2(\Omega_2)}\\
&+\left(B_{10,2}\frac{\partial^2\left(w_2^{(n+1)}-w_2^{(n)}\right)}{\partial x^2}\right.\\
&\left.+B_{11,2}\frac{\partial^2\left(w_2^{(n+1)}-w_2^{(n)}\right)}{\partial y^2},\frac{\partial^2\left(w_2^{(n+1)}-w_2^{(n)}\right)}{\partial y^2}\right)_{L_2(\Omega_2)}\\
&+\left(\left[B_{11,2}-B_{10,2}\right]\frac{\partial^2\left(w_2^{(n+1)}-w_2^{(n)}\right)}{\partial x\partial y},\frac{\partial^2\left(w_2^{(n+1)}-w_2^{(n)}\right)}{\partial x\partial y}\right)_{L_2(\Omega_2)}\\
&+\frac{kE}{h}\left(\psi(x,y)\left(w_2^{(n+1)}-w_2^{(n)}\right),\left(w_2^{(n+1)}-w_2^{(n)}\right)\right)_{L_2(\Omega_2)}\\
&=\frac{kE}{h}\left(\psi(x,y)\left(w_1^{(n)}-w_1^{(n-1)}\right)\right). \quad (25)
\end{aligned}$$

Given the definition of the function $\psi(x, y)$, we rewrite (23), (24) into following form:

$$\begin{aligned}
&\left(B_{11,1}\frac{\partial^2\left(w_1^{(n+1)}-w_1^{(n)}\right)}{\partial x^2}\right.\\
&\left.+B_{10,1}\frac{\partial^2\left(w_1^{(n+1)}-w_1^{(n)}\right)}{\partial y^2},\frac{\partial^2\left(w^{(n+1)}-w^{(n)}\right)}{\partial x^2}\right)_{L_2(\Omega_1)}\\
&+\left(B_{10,1}\frac{\partial^2\left(w_1^{(n+1)}-w_1^{(n)}\right)}{\partial x^2}\right.\\
&\left.+B_{11,1}\frac{\partial^2\left(w_1^{(n+1)}-w_1^{(n)}\right)}{\partial y^2},\frac{\partial^2\left(w_1^{(n+1)}-w_2^{(n)}\right)}{\partial y^2}\right)_{L_2(\Omega_1)}\\
&+\left(\left[B_{11,1}-B_{10,1}\right]\frac{\partial^2\left(w_1^{(n+1)}-w_1^{(n)}\right)}{\partial x\partial y},\right.\\
&\left.\frac{\partial^2\left(w_1^{(n+1)}-w_1^{(n)}\right)}{\partial x\partial y}\right)_{L_2(\Omega_1)}+\frac{kE}{h}\left\|\left(w_1^{(n+1)}-w_1^{(n)}\right)\right\|^2_{L_2(\Omega^*)}\\
&=\frac{kE}{h}\left(\left(w_2^{(n)}-w_2^{(n-1)}\right),\left(w_1^{(n+1)}-w_1^{(n)}\right)\right)_{L_2(\Omega^*)} \quad (26)\\
&\left(B_{11,2}\frac{\partial^2\left(w_2^{(n+1)}-w_2^{(n)}\right)}{\partial x^2}\right.\\
&\left.+B_{10,2}\frac{\partial^2\left(w_2^{(n+1)}-w_2^{(n)}\right)}{\partial y^2},\frac{\partial^2\left(w_1^{(n+1)}-w_1^{(n)}\right)}{\partial x^2}\right)_{L_2(\Omega_2)}\\
&+\left(B_{10,2}\frac{\partial^2\left(w_2^{(n+1)}-w_2^{(n)}\right)}{\partial x^2}\right.\\
&\left.+B_{11,2}\frac{\partial^2\left(w_2^{(n+1)}-w_2^{(n)}\right)}{\partial y^2},\frac{\partial^2\left(w_2^{(n+1)}-w_2^{(n)}\right)}{\partial y^2}\right)_{L_2(\Omega_2)}\\
&+\frac{kE}{h}\left\|\left(w_2^{(n+1)}-w_2^{(n)}\right)\right\|^2_{L_2(\Omega^*)}\\
&=\frac{kE}{h}\left(\left(w_1^{(n)}-w_1^{(n-1)}\right),\left(w_2^{(n+1)}-w_2^{(n)}\right)\right)_{L_2(\Omega^*)} \quad (27)
\end{aligned}$$

Using the Young's inequality [51], from (26), (27) and conditions of the theorem, we find:

$$\begin{aligned}
&D_1\left\|\Delta\left(w_1^{(n+1)}-w_1^{(n)}\right)\right\|^2_{L_2(\Omega^*)}\\
&\quad+\frac{kE}{h}\left\|\left(w_1^{(n+1)}-w_1^{(n)}\right)\right\|^2_{L_2(\Omega^*)}\\
&\le\frac{kE}{2h}\left\|\left(w_2^{(n)}-w_2^{(n-1)}\right)\right\|^2_{L_2(\Omega^*)}\\
&\quad+\frac{kE}{2h}\left\|\left(w_1^{(n+1)}-w_1^{(n)}\right)\right\|^2_{L_2(\Omega^*)},\\
&D_2\left\|\Delta\left(w_2^{(n+1)}-w_2^{(n)}\right)\right\|^2_{L_2(\Omega_2)}\\
&\quad+\frac{kE}{h}\left\|\left(w_2^{(n+1)}-w_2^{(n)}\right)\right\|^2_{L_2(\Omega^*)}\\
&\le\frac{kE}{h}\left\|\left(w_1^{(n)}-w_1^{(n-1)}\right)\right\|^2_{L_2(\Omega^*)}\\
&\quad+\frac{kE}{2h}\left\|\left(w_2^{(n+1)}-w_2^{(n)}\right)\right\|^2_{L_2(\Omega^*)}.
\end{aligned}$$

Finally, we obtain:

$$D_1\left\|\Delta\left(w_1^{(n+1)}-w_1^{(n)}\right)\right\|^2_{L_2(\Omega^*)}$$

$$+\frac{kE}{2h}\left\|\left(w_2^{(n)}-w_2^{(n-1)}\right)\right\|^2_{L_2(\Omega^*)}$$
$$\le \frac{kE}{2h}\left\|\left(w_2^{(n+1)}-w_2^{(n)}\right)\right\|^2_{L_2(\Omega^*)}, \quad (28)$$
$$D_2\left\|\Delta\left(w_1^{(n+1)}-w_1^{(n)}\right)\right\|^2_{L_2(\Omega^*)}$$
$$+\frac{kE}{2h}\left\|\left(w_2^{(n+1)}-w_2^{(n)}\right)\right\|^2_{L_2(\Omega^*)}$$
$$\le \frac{kE}{2h}\left\|\left(w_1^{(n)}-w_1^{(n-1)}\right)\right\|^2_{L_2(\Omega^*)}. \quad (29)$$

We rewrite (28) and (29) into the following form:

$$D_1\left\|\Delta\left(w_1^{(n+1)}-w_1^{(n)}\right)\right\|^2_{L_2(\Omega^*)}$$
$$+\frac{kE}{2h}\left\|\left(w_1^{(n+1)}-w_1^{(n)}\right)\right\|^2_{L_2(\Omega^*)}$$
$$\le (1-\alpha)\frac{kE}{2h}\left\|\left(w_2^{(n)}-w_2^{(n-1)}\right)\right\|^2_{L_2(\Omega^*)}$$
$$+\alpha\frac{kE}{2h}\left\|\left(w_2^{(n)}-w_2^{(n-1)}\right)\right\|^2_{L_2(\Omega^*)}, \quad (30)$$
$$D_2\left\|\Delta\left(w_2^{(n+1)}-w_2^{(n)}\right)\right\|^2_{L_2(\Omega_2)}$$
$$+\frac{kE}{2h}\left\|\left(w_2^{(n+1)}-w_2^{(n)}\right)\right\|^2_{L_2(\Omega^*)}$$
$$\le (1-\alpha)\frac{kE}{2h}\left\|\left(w_1^{n}-w_1^{(n-1)}\right)\right\|^2_{L_2(\Omega^*)}$$
$$+\alpha\frac{kE}{2h}\left\|\left(w_1^{(n)}-w_1^{(n-1)}\right)\right\|^2_{L_2(\Omega^*)}. \quad (31)$$

where $\alpha \in R^1, 0 < \alpha < 1$.

Furthermore, we implement the Friedrichs' inequality [51] in the following manner. There exists a constant $c_i \in R^{1,}$ such that$\forall f(x, y) \in \dot{W}_2^2(\Omega_i)$, $i = 1, 2$ and the following inequalities:

$$\|f\|^2_{L_2(\Omega*)} \le c_i \|\Delta f\|^2_{L_2(\Omega*)} \le c_i \|\Delta f\|^2_{L_2(\Omega)}, \quad i = 1, 2, \quad (32)$$

where it is believed that $\Omega^* \subseteq \Omega_i$ and satisfies the conditions of applicability of the Friedrichs' inequality. Then, taking into account (32), the inequalities (30) and (31) are reduced to the following ones:

$$D_1\left\|\Delta\left(w_1^{(n+1)}-w_1^{(n)}\right)\right\|^2_{L_2(\Omega_i)}$$
$$+\frac{kE}{2h}\left\|\left(w_1^{(n+1)}-w_1^{(n)}\right)\right\|^2_{L_2(\Omega^*)}$$
$$\le (1-\alpha)\frac{kE}{2h}\left\|\left(w_2^{(n)}-w_2^{(n-1)}\right)\right\|^2_{L_2(\Omega^*)}$$
$$+\frac{\alpha C_2 kE}{D_2 2h}D_1\left\|\Delta\left(w_1^{(n+1)}-w_1^{(n)}\right)\right\|^2_{L_2(\Omega)}, \quad (33)$$

$$D_2\left\|\Delta\left(w_2^{(n+1)}-w_2^{(n)}\right)\right\|^2_{L_2(\Omega_2)}$$
$$+\frac{kE}{2h}\left\|\left(w_2^{(n+1)}-w_2^{(n)}\right)\right\|^2_{L_2(\Omega^*)}$$
$$\le (1-\alpha)\frac{kE}{2h}\left\|\left(w_1^{n}-w_1^{(n-1)}\right)\right\|^2_{L_2(\Omega^*)}$$
$$+\frac{\alpha C_1 kE}{D_1 2h}D_1\left\|\Delta\left(w_1^{(n+1)}-w_1^{(n)}\right)\right\|^2_{L_2(\Omega)}. \quad (34)$$

In inequalities (33) and (34) we take α that fulfills the following conditions

$$\frac{\alpha C_2 kE}{2hD_2} < 1, \frac{\alpha C_1 kE}{2hD_1} < 1, 0 < \alpha < 1,$$

and

$$\rho = \max\left\{(1-\alpha), \frac{\alpha C_2 kE}{2hD_2}, \frac{\alpha C_1 kE}{2hD_1}\right\}.$$

Obviously, we consider the case $0 < \rho < 1$. Now the inequalities (33) and (34) can be transformed into the following form:

$$D_1\left\|\Delta\left(w_1^{(n+1)}-w_1^{(n)}\right)\right\|^2_{L_2(\Omega_1)}$$
$$+\frac{kE}{2h}\left\|\left(w_1^{(n+1)}-w_1^{(n)}\right)\right\|^2_{L_2(\Omega^*)}$$
$$\le \rho\left\{D_2\left\|\Delta\left(w_2^{(n)}-w_2^{(n-1)}\right)\right\|^2_{L_2(\Omega_2)}\right.$$
$$\left.+\frac{kE}{2h}\left\|\left(w_2^{(n)}-w_2^{(n-1)}\right)\right\|^2_{L_2(\Omega^*)}\right\}, \quad (35)$$
$$D_2\left\|\Delta\left(w_2^{(n+1)}-w_2^{(n)}\right)\right\|^2_{L_2(\Omega_2)}$$
$$+\frac{kE}{2h}\left\|\left(w_2^{(n+1)}-w_2^{(n)}\right)\right\|^2_{L_2(\Omega^*)}$$
$$\le \rho\left\{D_1\left\|\Delta\left(w_1^{(n)}-w_1^{(n-1)}\right)\right\|^2_{L_2(\Omega_1)}\right.$$
$$\left.+\frac{kE}{2h}\left\|\left(w_1^{(n)}-w_1^{(n-1)}\right)\right\|^2_{L_2(\Omega^*)}\right\}. \quad (36)$$

Summing (35) and (36), we get:

$$\left\{D_1\left\|\Delta\left(w_1^{(n+1)}-w_1^{(n)}\right)\right\|^2_{L_2(\Omega_1)}\right.$$
$$+D_2\left\|\Delta\left(w_2^{(n+1)}-w_2^{(n)}\right)\right\|^2_{L_2(\Omega_2)}$$
$$+\frac{kE}{2h}\left\|\left(w_1^{(n+1)}-w_1^{(n)}\right)\right\|^2_{L_2(\Omega^*)}$$
$$\left.+\frac{kE}{2h}\left\|\left(w_2^{(n+1)}-w_2^{(n)}\right)\right\|^2_{L_2(\Omega^*)}\right\}$$
$$\le \rho\left\{D_1\left\|\Delta\left(w_1^{(n)}-w_1^{(n-1)}\right)\right\|^2_{L_2(\Omega_1)}\right.$$

$$+D_2\left\|\Delta\left(w_2^{(n)}-w_2^{(n-1)}\right)\right\|^2_{L_2(\Omega_1)}$$
$$+\frac{kE}{2h}\left\|\left(w_1^{(n)}-w_1^{(n-1)}\right)\right\|^2_{L_2(\Omega^*)}$$
$$+\frac{kE}{2h}\left\|\left(w_2^{(n)}-w_2^{(n-1)}\right)\right\|^2_{L_2(\Omega^*)}\Bigg\}, \tag{37}$$

or

$$\left\|\bar{w}^{(n+1)}-\bar{w}^{(n)}\right\|^2_H \le \rho\left\|\bar{w}^{(n)}-\bar{w}^{(n-1)}\right\|^2_H, \tag{38}$$

where $\bar{w}^{(n)}=(w_1^{(n)},w_2^{(n)})$, H—normed space with the norm equivalent to the norm of $\dot{W}_2^2(\Omega_1)\times\dot{W}_2^2(\Omega_2)$ and determining the left (or right) side of the inequality (36). From (38) we have:

$$\left\|\bar{w}^{(n+1)}-\bar{w}^{(n)}\right\|_H \le \rho\left\|\bar{w}^{(n)}-\bar{w}^{(n-1)}\right\|_H,$$
$$\rho_1=\sqrt{\rho}<1,\ \left\|\bar{w}^{(n+1)}-\bar{w}^{(n)}\right\|_H\le\theta\rho_1^n,$$

where $\theta=\left\|\bar{w}^{(1)}-\bar{w}^0\right\|_H$.

Then, for any positive integer we obtain:

$$\left\|\bar{w}^{(n+p)}-\bar{w}^{(n)}\right\|_H \le \left\|\bar{w}^{(n+p)}-\bar{w}^{(n+p-1)}\right\|_H$$
$$+\left\|\bar{w}^{(n+p-1)}-\bar{w}^{(n+p-2)}\right\|_H$$
$$+\left\|\bar{w}^{(n+1)}-\bar{w}^{(n)}\right\|_H\le\theta\rho_1^{(n+p-1)}$$
$$+\theta\rho_1^{(n+p-2)}+\ldots+\theta\rho_1^{(n)}=\frac{\theta\left(\rho_1^{(n)}+\rho_1^{(n+p)}\right)}{1-\rho_1}$$
$$\le\frac{\theta\rho_1^{(n)}}{1-\rho_1}. \tag{39}$$

From (39), the fundamental sequence $\left\{\bar{w}^{(n)}\right\}$ follows, and, owing to the completeness of H, a convergence $\left\{\bar{w}^{(n)}\right\}$ to a certain function $\bar{w}^*=(w_1^*,w_2^*)$ in H is achieved.

Thus, by virtue of equivalence of norms in the spaces H and $\dot{W}_2^2(\Omega_1)\times\dot{W}_2^2(\Omega_2)$ we get:

$$\lim_{n\to\infty}\left\|w_i^n-w_i^*\right\|_{\dot{W}_2^2(\Omega_i)}=0,\quad i=1,2, \tag{40}$$

We rewrite systems (22), (23) into the following form:

$$\left(B_{11,1}\frac{\partial^2 w_1^{(n+1)}}{\partial x^2}+B_{10,1}\frac{\partial^2 w_1^{(n+1)}}{\partial y^2},\frac{\partial^2\varphi_1}{\partial x^2}\right)_{L_2(\Omega_1)}$$
$$+\left(B_{10,1}\frac{\partial^2 w_1^{(n+1)}}{\partial x^2}+B_{11,1}\frac{\partial^2 w_1^{(n+1)}}{\partial y^2},\frac{\partial^2\varphi_1}{\partial y^2}\right)_{L_2(\Omega_1)}$$
$$+\left(\left[B_{11,1}-B_{10,1}\right]\frac{\partial^2 w_1^{(n+1)}}{\partial x\partial y}\frac{\partial^2\varphi_1}{\partial x\partial y}\right)_{L_2(\Omega_1)}$$
$$+\frac{kE}{h}\left(\psi(x,y)\,w_1^{(n+1)},\varphi_1\right)_{L_2(\Omega_1)}=(q_1\varphi_1)_{L_2(\Omega_1)}$$
$$+\frac{kE}{h}\left(\psi(x,y)\left[w_1^{(n)}+h_1\right],\varphi_1\right)_{L_2(\Omega^*)}, \tag{41}$$
$$\left(B_{11,2}\frac{\partial^2 w_1^{(n+1)}}{\partial x^2}+B_{10,2}\frac{\partial^2 w_2^{(n+1)}}{\partial y^2},\frac{\partial^2\varphi_2}{\partial x^2}\right)_{L_2(\Omega_2)}$$
$$+\left(B_{10,2}\frac{\partial^2 w_2^{(n+1)}}{\partial x^2}+B_{11,2}\frac{\partial^2 w_2^{(n+1)}}{\partial y^2},\frac{\partial^2\varphi_2}{\partial y^2}\right)_{L_2(\Omega_2)}$$
$$+\left(\left[B_{11,2}-B_{10,2}\right]\frac{\partial^2 w_2^{(n+1)}}{\partial x\partial y}\frac{\partial^2\varphi_2}{\partial x\partial y}\right)_{L_2(\Omega_2)}$$
$$+\frac{kE}{h}\left(\psi(x,y)\,w_2^{(n+1)},\varphi_2\right)_{L_2(\Omega_2)}$$
$$=(q_2[1-\psi(x,y)],\varphi_2)_{L_2(\Omega_2)}$$
$$+\frac{kE}{h}\left(\psi(x,y)\left[w_1^{(n)}+h_1\right],\varphi_1\right)_{L_2(\Omega^*)},$$
$$\forall\varphi_1\in\dot{W}_2^2(\Omega_1),\quad\forall\varphi_2\in\dot{W}_2^2(\Omega_2). \tag{42}$$

The condition (40) allows the Eqs. (41), (42) to reach the limit for $n\to\infty$ and thus the following relations are obtained:

$$\left(B_{11,1}\frac{\partial^2 w_1^*}{\partial x^2}+B_{10,1}\frac{\partial^2 w_1^*}{\partial y^2},\frac{\partial^2\varphi_1}{\partial x^2}\right)_{L_2(\Omega_1)}$$
$$+\left(B_{10,1}\frac{\partial^2 w_1^*}{\partial x^2}+B_{11,1}\frac{\partial^2 w_1^*}{\partial y^2},\frac{\partial^2\varphi_1}{\partial y^2}\right)_{L_2(\Omega_1)}$$
$$+\left(\left[B_{11,1}-B_{10,1}\right]\frac{\partial^2 w_1^*}{\partial x\partial y}\frac{\partial^2\varphi_1}{\partial x\partial y}\right)_{L_2(\Omega_1)}$$
$$+\frac{kE}{h}\left(\psi(x,y)\,w^*,\varphi_1\right)_{L_2(\Omega_1)}=(q_1\varphi_1)_{L_2(\Omega_1)}$$
$$+\frac{kE}{h}\left(\psi(x,y)\left[w_2^*+h_1\right],\varphi_1\right)_{L_2(\Omega^*)}, \tag{43}$$
$$\left(B_{11,2}\frac{\partial^2 w_1^*}{\partial x^2}+B_{10,2}\frac{\partial^2 w_1^*}{\partial y^2},\frac{\partial^2\varphi_1}{\partial x^2}\right)_{L_2(\Omega_2)}$$
$$+\left(B_{10,2}\frac{\partial^2 w_1^*}{\partial x^2}+B_{11,2}\frac{\partial^2 w_1^*}{\partial y^2},\frac{\partial^2\varphi_1}{\partial y^2}\right)_{L_2(\Omega_2)}$$
$$+\left(\left[B_{11,2}-B_{10,2}\right]\frac{\partial^2 w_1^*}{\partial x\partial y}\frac{\partial^2\varphi_1}{\partial x\partial y}\right)_{L_2(\Omega_2)}$$
$$+\frac{kE}{h}\left(\psi(x,y)\,w_2^*,\varphi_2\right)_{L_2(\Omega_2)}$$

$$= (q_2 [1 - \psi(x, y)], \varphi_2)_{L_2(\Omega_2)} + \frac{kE}{h} \left(\psi(x, y) \left[w_1^* + h_1\right], \varphi_1\right)_{L_2(\Omega^*)}, \quad (44)$$

which, in turn, proves the second conclusion of Theorem 3. □

4 Contact interaction of two elastic rectangular plates

Below some examples of the iterative procedure (22) used to study contact problems for two rectangular plates are presented ($E_1 = E_2 = E = const$, $\nu_1 = \nu_2 = 0.3$).

We introduce the following dimensionless notation:

$$\overline{x} = \frac{x}{a}, \overline{y} = \frac{y}{b}, \overline{w}_j = \frac{w_j}{h}, \overline{h}_1 = \frac{h_1}{h}, \lambda_1 = \frac{a}{h}, \lambda_2 = \frac{b}{h}, \lambda = \frac{a}{b},$$
$$\overline{q}_j = 12(1 - \nu^2)\lambda_1^2\lambda_2^2 \frac{q_j}{E}, \overline{k} = 12(1 - \nu^2)\lambda_1^2\lambda_2^2 k. \quad (45)$$

Then, the iterative procedure, including dimensionless variables, has the following form (dashes are omitted):

$$A_1(w_1^{(n+1)}(x, y)) + k w_1^{(n+1)} \psi(x, y) = q + k(w_2^{(n)} + h_1)\psi(x, y),$$
$$A_2(w_2^{(n+1)}(x, y)) + k w_2^{(n)} \psi(x, y) = q(1 - \psi(x, y)) + k(w_1^{(n)} - h_1)\psi(x, y), \quad (46)$$

where $q = q_1 = q_2$

Operators A_j are derived for both linear and nonlinear problems. For example, for a linear problem we have

$$A_i = \left(\frac{1}{\lambda^2}\right) \frac{\partial^4 w_i(x, y)}{\partial x^4} + 2 \frac{\partial^4 w_i(x, y)}{\partial x^2 \partial y^2} + \lambda^2 \frac{\partial^4 w_i(x, y)}{\partial y^4}, i = 1, 2$$

4.1 Contact interaction of two square plates of constant thickness

Let us assume that both plates have constant thickness and that $a/h = 10$. The stiffness coefficient of transverse compression in the contact zone $k = 4 \cdot 10^3$. Plates are square, $\lambda = a/b = 1$. The applied load is uniformly distributed over the plate surface.

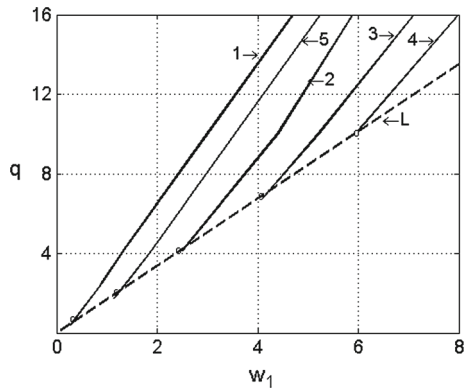

Fig. 2 Dependence $q(w_1)$ for the boundary condition 5

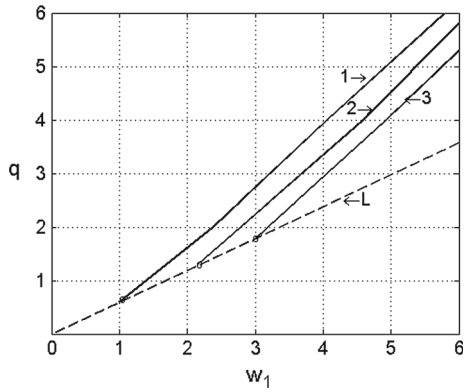

Fig. 3 Dependence $q(w_1)$ for the boundary condition 4

We investigate the impact of the gap between plates h_1 and the boundary conditions 4, 5 on the stress–strain state (SSS). Graphs of $q(w_1)$ are presented in Fig. 2 (for the boundary condition 5), and Fig. 3 (for the boundary condition 4 for both plates).

Circles indicate the specified values of deflection for which the contact between plates is established. In Fig. 2, 3 the numbers correspond to the following distances between plates: $1 - h_1 = 1 \cdot 10^{-4}$; $2 - h_2 = 2 \cdot 10^{-2}$; $3 - h_3 = 4 \cdot 10^{-2}$; $4 - h_4 = 6 \cdot 10^{-2}$; $5 - h_5 = 1 \cdot 10^{-2}$. Dashed lines indicate the results regarding one-layer plates.

The figures show the effect of the size of the gap between plates on the function $q(w_1)$. The curve 1 in Fig. 2 and Fig. 3 presents the results for a two-layer plate with a gap of 100 times smaller size than the one considered for the curve 5. In this case, during the initial stages of loading, two-layer plate carries two times higher load than does the one-layer plate. Comparing the dependences shown in Figs. 2 and 3, it can

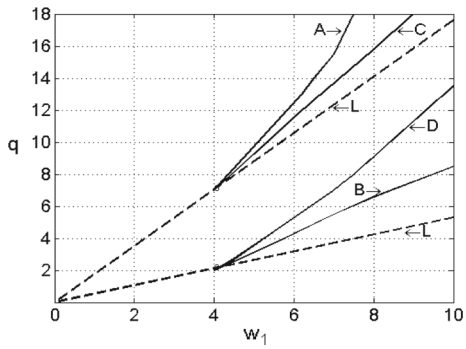

Fig. 4 Dependence $q(w_1)$ for different types of boundary conditions. ($h_1 = 0,02$)

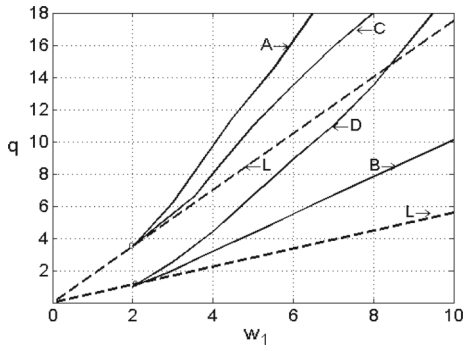

Fig. 5 Dependence $q(w_1)$ for different types of boundary conditions ($h_1 = 0,04$)

be noticed that for the boundary condition 4 the difference between results obtained for different gap sizes is greater than in the case of the boundary condition 5. Similar phenomenon can be observed for the contact interaction of two plates with the boundary condition 4, shown in Fig. 3.

Let us consider the influence of the boundary condition type on $q(w_1)$. These results are presented in Figs. 4 and 5 for four types of boundary conditions for a three-layer system of square plates with a clearance between them equal to $h_1 = 0.02$ and $h_1 = 0.04$. Curve *A* corresponds to a set of boundary conditions ((5)–(5)), curve B to a set of boundary conditions ((4)–(4)), curve *C* to the set of boundary conditions ((5)–(4)), and the curve *D* to the set of boundary conditions ((4)–(5)). Dashed lines in both figures indicate the results for the one-layer plates.

Based on the analysis of the above results, it can be concluded that the boundary conditions of the upper plate substantially influence the SSS of the whole system. Thus, the $q(w_1)$ curves are similar for the

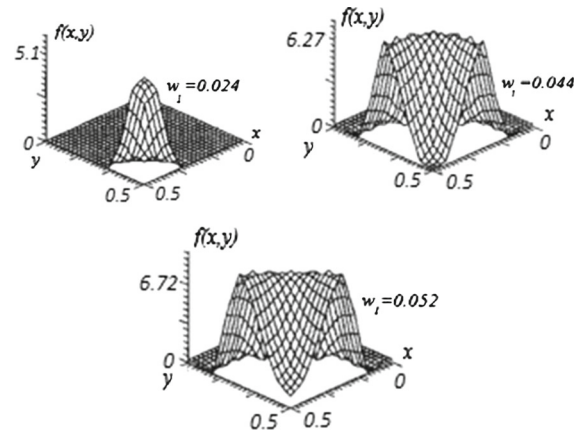

Fig. 6 Contact pressure distribution between layers for boundary conditions (4)–(5)

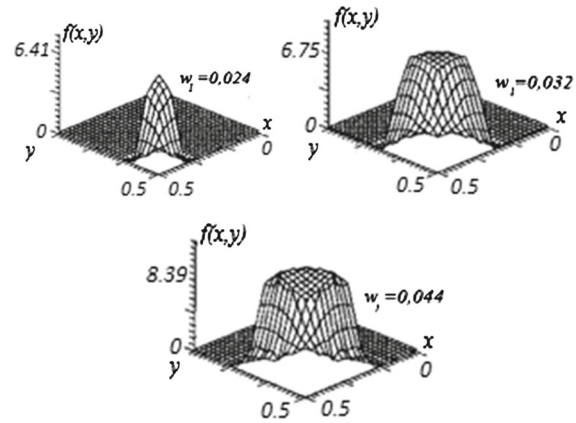

Fig. 7 Contact pressure distribution between layers for boundary conditions (5)–(5)

clamped–clamped ((5)–(5)) and clamped–simply supported ((5)–(4)) combinations as well as for combinations ((4)–(4)) and ((4)–(5)).

Distribution of contact pressure between layers for three types of combinations of boundary conditions for the gap $h_1 = 0,02$ is shown in Fig. 6—for boundary conditions ((4)–(5)), Fig. 7—for boundary conditions ((5)–(5)) and in Fig. 8—for boundary conditions ((5)–(4)). The diagrams show the contact pressure for a quarter of the area in view of symmetry of the solution. The values of deflection for the plates for which the contact pressure diagrams were obtained are also presented in Figs. 6, 7 and 8.

The above figures clearly indicate that the nature and the magnitude of the contact pressure depends on the type of boundary conditions. Maximum contact pressure is found for the diagonals of the plates. Increasing

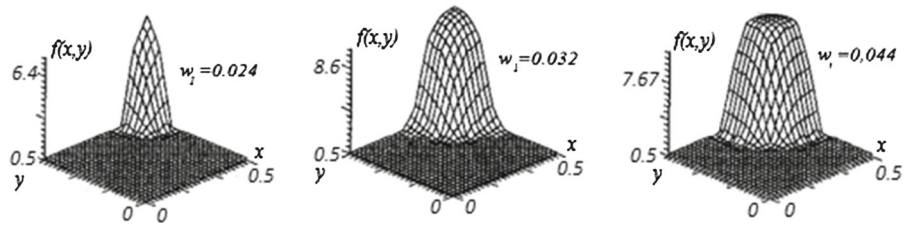

Fig. 8 Contact pressure distribution between layers for boundary conditions (5)–(4)

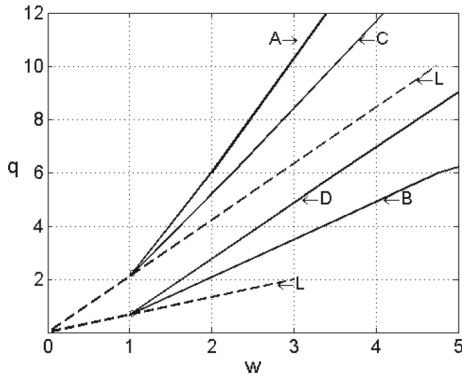

Fig. 9 Dependence $q(w_1)$ for different boundary conditions for $h_1 = 0.01$ (see text for more details)

load results in pressure that greatly varies on the boundaries of the contact zones, where the characteristic value of max $q_k(x, y)$ is observed for the contact problems of the plate theory. For the pair of the boundary conditions ((5)–(4)), such a pattern is not observed.

Although at the first glance the problem seems to be easy to solve, obtaining the solution with the use of conventional approaches is rather difficult. Indeed, for this purpose, a system of 8th order differential equations should be solved along with kinematic conditions of contact $w_1 = w_2 + h_1$ and defined boundaries of the contact zone. If the transverse deformation of layers in the contact zone is not taken into account, the concentrated shear forces at the zone boundaries are also unknown.

4.2 Contact interaction of two square plates with varying thickness

Let the thickness of two plates vary according to the following formula:

$$h(x, y) = 1.0 + 0.1 \cdot \sin \pi x \cdot \sin \pi y. \tag{47}$$

The gap between the plates at the edge of the system is fixed $h_1 = 0.01$, whereas according to the plane (x, y) it is a variable quantity. We will consider the problem for four combinations of boundary conditions: A—the upper and lower plates are clamped—boundary conditions (5)–(5); B—both plates are simply supported—boundary conditions (4)–(4); C—the upper plate is clamped—boundary condition (5), and the lower is simply supported—boundary condition (4); D—the upper plate is simply supported—boundary condition (5), and the lower is clamped—boundary condition (4).

The graph of $q(w_1)$ is presented in Fig. 9. Dashed lines correspond to the results obtained for one-layer plates in linear consideration (L is the lower plate). Circles in the plot of $q(w_1)$ indicate the deflection for which the contact between plates is established.

The analysis of the dependency $q(w_1)$ shows that the main factor affecting $q(w_1)$ is the type of the boundary condition of the upper plate. For the same load, two times bigger contact has been observed for the case the boundary condition (5), than for the condition (4). Note also that for high loads the difference is smaller in graphs A–C than in graphs B–D.

The nature of changes of contact pressure $f(x, y)$ zones for the simply supported plate—type B and the clamped plate—type A on the plate contour for $h_1 = 0.001$ is shown in Fig. 10 and 11, respectively.

With the increase in the area of contact pressure (from $w_1 = 0.015$ to $w_1 = 0.04$), the character of the pressure significantly changes. There are "boundary peaks", indicating more complex, wavy nature of contact. Here the forces concentrated at the border appear significantly more vivid than for plates of constant thickness.

4.3 Interplay of physically nonlinear two square plates of constant thickness

Let two-layer plates be made of different materials having identical elastic moduli, but different stress–strain $\sigma_i^{(i)}(e_i^{(i)})$ diagrams. Boundary conditions (4) and (5)

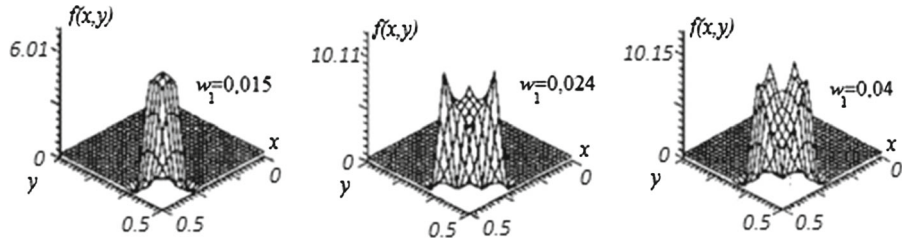

Fig. 10 Contact pressure zones for different w_1 (simply supported plate)

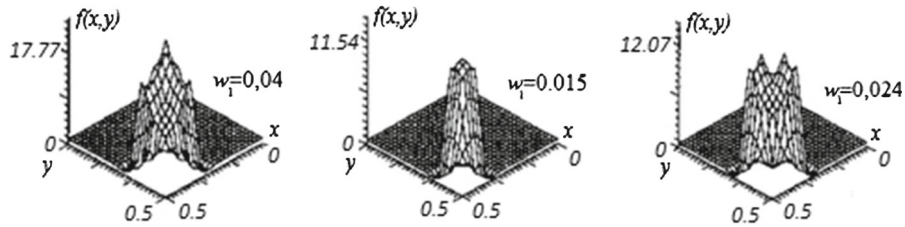

Fig. 11 Contact pressure zones for different w_1 (clamped plate)

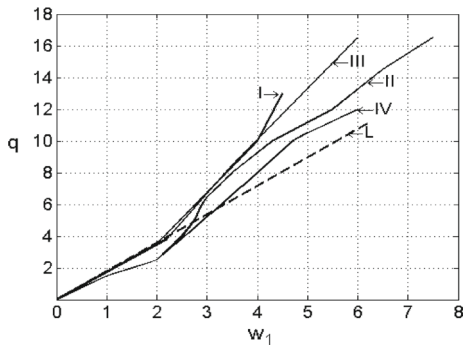

Fig. 12 Functions $q(w_1)$ for boundary conditions (5)–(5)

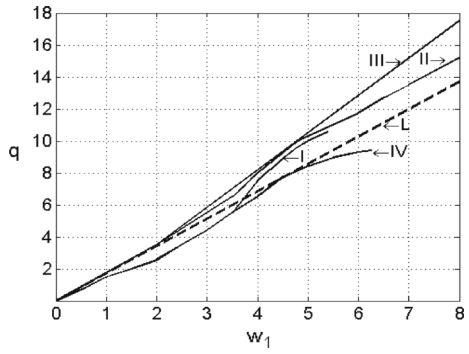

Fig. 14 Functions $q(w_1)$ for boundary conditions (5)–(4)

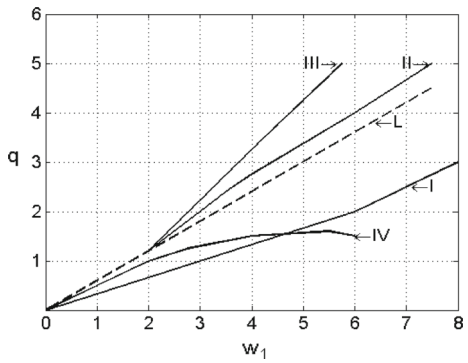

Fig. 13 Functions $q(w_1)$ for boundary conditions (4)–(4)

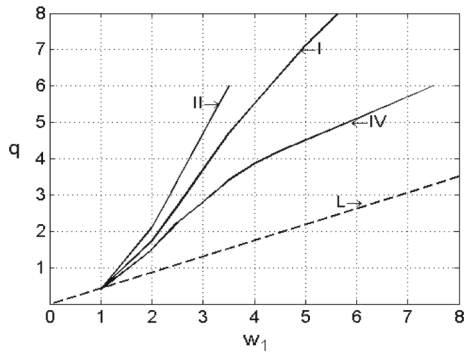

Fig. 15 Functions $q(w_1)$ for boundary conditions (4)–(5)

are considered. In the following examples, two types of diagrams $\sigma_i^{(i)}(e_i^{(i)})$are studied. Nonlinear stress is governed by the following equation

$$\sigma_i = \sigma_S \left[1 - \exp(-e_i/e_S)\right], \tag{48}$$

where: $\sigma_s = 1023$ bar, $G_0 = 0.3483 \times 10^{-6}$ bar, $e_{is} = 0.98 \times 10^{-3}$, $a/h = 10$, $e_s = e_{is}(a/h) = 0.098$, $\nu_0 = 0.28$.

Linear stress obeys the Hooke's law, i.e.

$$\sigma_i^{(i)} = 3G_0(e_i^{(i)}). \tag{49}$$

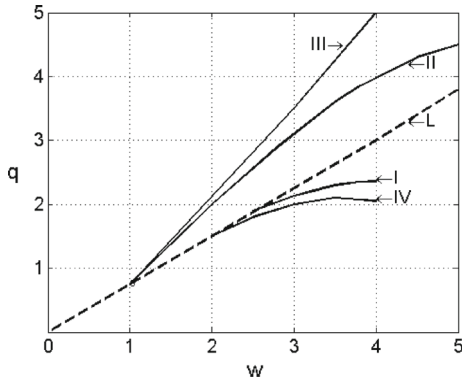

Fig. 16 Functions $q(w)$ for different boundary conditions ($h_1 = 0.01$)

The stiffness coefficient of transverse compression of a plate in a contact zone $k = 1000$. Dependences $q(w_1)$ for the considered problems are given in Figs. 12, 13, 14 and 15 for $h_1 = 0.02$, and for $h_1 = 0.01$—in Fig. 16.

Each of the above four figures describes "load—deflection at the center of the plate" dependence for one type of boundary conditions depicted in the drawing. Roman numerals denote the corresponding solution to problems, depending on the distribution of material diagrams for each of the plates: I—the upper plate ($\sigma_i(e_i)$—nonlinear), the lower plate ($\sigma_i(e_i)$—linear); II—the upper plate ($\sigma_i(e_i)$—linear), the lower plate ($\sigma_i(e_i)$—nonlinear); III—the upper and the lower plates ($\sigma_i(e_i)$—linear); IV—the upper plate and the lower plates ($\sigma_i(e_i)$—nonlinear).

Distribution of elastic–plastic zones for the 1/4 of the upper plate of a two-layer system is reported in Fig. 17 for $h_1 = 0.02$, in Fig. 18 for $h_1 = 0.01$ and

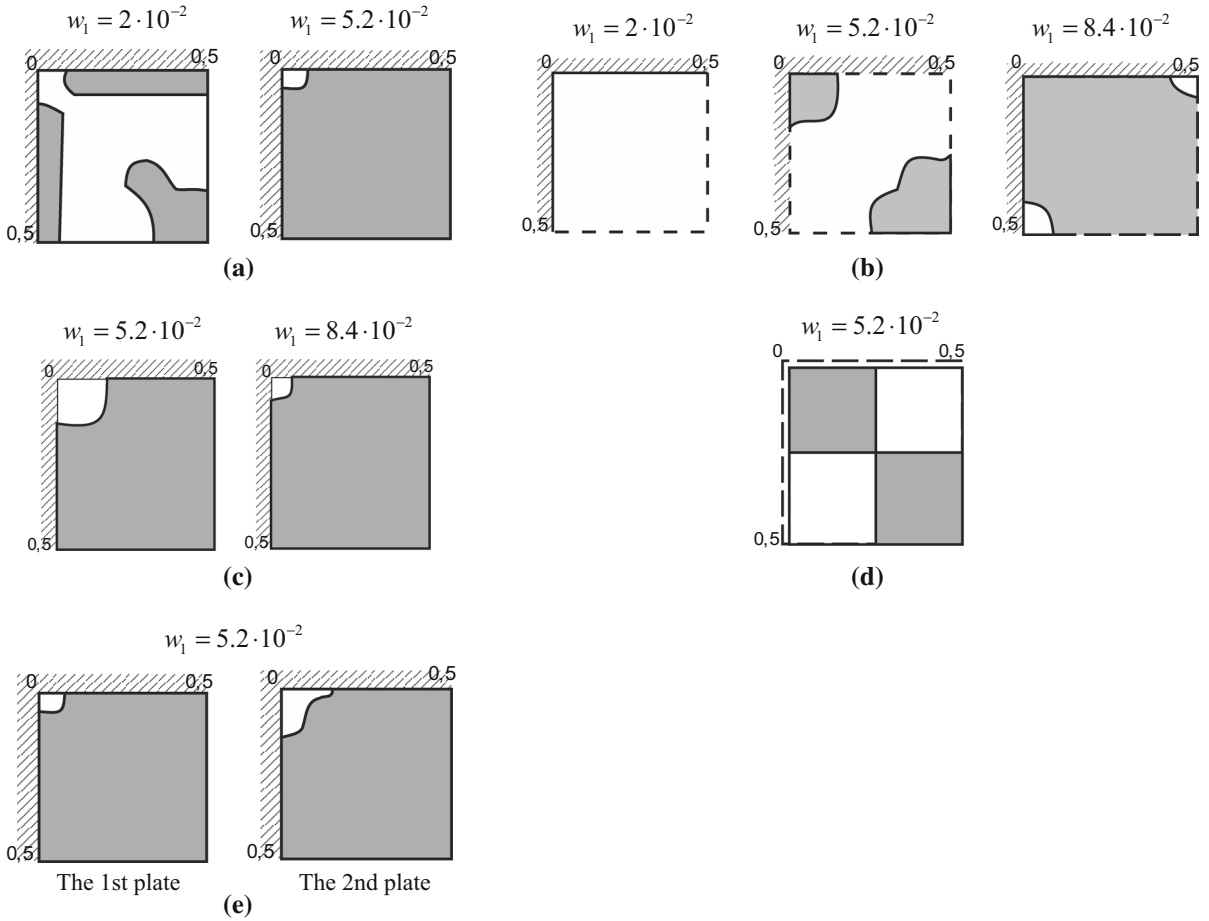

Fig. 17 Elastic–plastic zones distribution for the quarter of a plate: **a** First plate; problem C_I; **b** First plate; problem C_{II}; **c** Second plate; problem A_{II}; **d** First plate; problem B_{II}; **e** problem A_{IV} for two plates

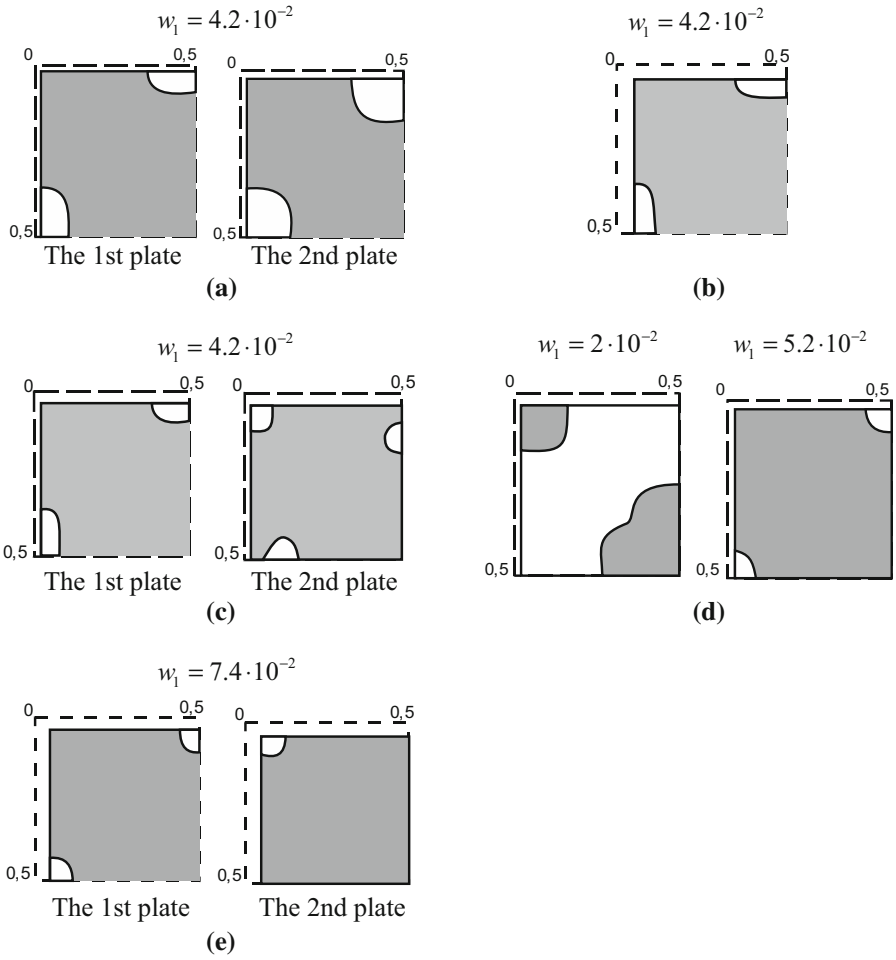

Fig. 18 Elastic and plastic zones distribution: **a** problem B_{IV}; **b** First plate; problem D_I; **c** problem D_{II}; **d** First plate; problem L

in Fig. 19 for $h_1 = 0.01$. Plastic zones are indicated in gray color. In the same figures the following parameters, for which the calculations of a design are made, are specified: deflection at the center of the upper plate $w_1(0.5, 0.5)$, the value of the gap between the plates h_1, the type of nonlinearity and boundary conditions. The crosshatched contour indicates the boundary condition (5), while the dashed one is associated with the boundary condition (4).

The above-mentioned considerations are made for the clearance equal to $h_1 = 0.02$. In the case when the upper plate is nonlinear (Problem I), and the boundary conditions (5)–(4) are taken into account, small deflections plastic zones are located along the perimeter of the plate and at its center. With increasing deflection of the zones, elastoplastic deformation occupies almost the entire area of the plate, except for the corners (Figure 17a). For the same boundary conditions, for the linear upper plate—Problem II (see Figure 17b), the distribution of elastic–plastic zones is different. In this case, zones of elastoplastic deformation are located in the middle and on the corners of the plate. Note that with the increase in the deflection, plastic zones tend to occupy almost the whole area of the plate, and rigid zones can be observed on the corners and in the middle part of the plate. Note also that the plastic deformation zone has a larger deflection value than it was in Problem I. Thus, it can be concluded that the change in the type of a problem (I–II) significantly affects the arrangement of the elastic–plastic deformation zones.

For a case when both plates are clamped, boundary conditions (5)–(5) are considered and both plates are physically nonlinear (Problem IV), the zones of elasto-plastic deformations given in Fig. 17e qualitatively coincide for the first and the second plate, what

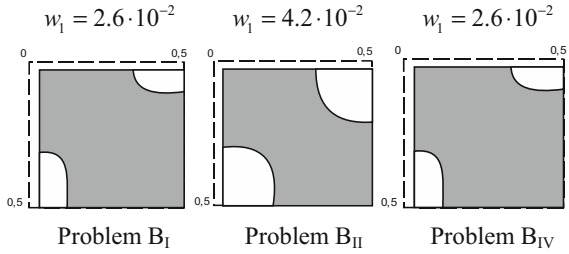

Fig. 19 Elastic–plastic deformations the First plate for different w_1 and different B problems

follows from compatibility of both the boundary conditions and the type of the plate.

In the case when the type of the problem changes and becomes "asymmetrical," i.e., the upper plate is linear and the lower one—nonlinear (Problem II), zones of elastic–plastic deformations for the 2nd plate are as shown in Fig. 17c. These zones are qualitatively consistent with the results for the 1st plate (for the Problem C_I). Thus, for the lower (second) plate, the main condition of a qualitative arrangement of plastic zones is the type of the plate: physically linear or physically nonlinear.

For the combination of boundary conditions (4)–(4), in the case when the upper plate is linear, and the bottom is nonlinear, the distribution of plastic deformation zones of the first plate, shown in Fig. 18a, coincides in size with the zones of elastic deformation.

As the distance between the plates $h_1 = 0.01$ decreases, the following results are obtained. For the boundary conditions (5)–(4), the size and arrangement of zones of the elastic–plastic deformation do not depend on the type of the problem. This is confirmed by Fig. 18b which shows the results for the Problem I and Figure 18c—for the Problem II, respectively. With the increase in the deflection in the Problem II (Fig 18c), the elastic zones become reduced for both plates and are located in different places—for the 1st plate in the middle part, and for the 2nd—on the corners.

For the case when both plates are simply supported (4)–(4) and nonlinearity of both plates and the gap $h_1 = 0.02$ is provided, the zones of elastic–plastic deformation of both plates qualitatively coincide with the results shown in Fig. 18a. The solution for one plate with the boundary conditions (4) is given in Fig. 18d. The results are qualitatively similar to the results for the 1st plate, shown in Fig. 17b.

Figure 19 presents zones of elastic–plastic deformation of the first plate for one type of boundary conditions (4)–(4), but with different types of the considered plates. Note that the results are qualitatively identical. For the type II the arrangement of zones of elastic–plastic deformation differs from the results for the other two cases. This is due to difference in the problem formulation for the upper plate. For Problem II the upper plate is physically linear.

5 Concluding remarks

The following main conclusions of our research can be formulated

1. We present an iterative procedure of the solution to structurally nonlinear problems for two plates being in contact with each other. Each of the plates can be described with a mathematical model combining displacements and deformations in the form of von Kármán, i.e., geometrical nonlinearity is considered. Taking into account the relationship between stress and strain, the model considers also physical nonlinearity. In other words both geometrical and physical nonlinearities can be taken into account.
2. The theorem of convergence of the iterative procedure proposed by the authors is proved for the boundary conditions of clamping. Justification of convergence of the iterative algorithm can be easily extended in the case of other boundary conditions. For example, the proposed scheme of proof remains unchanged if one or both of the contacting plates is simply supported.
3. The proposed iterative algorithm can be used in problems of contacting plates, taking into account physical nonlinearity (combined with the method of elastic solutions, the scheme of the proof remains unchanged).
4. Each of two contacting plates that are considered in the work is one-layer, but the proposed algorithm, can be extended to the case where each of plates is multilayer.

Acknowledgments This work has been supported by the Polish National Science Centre, MAESTRO 2, No. 2012/04/A/ST8/00738. The project has been also supported by the Grants RFBR 16-08-01108a and RFBR 16-01-00721a.

References

1. Hertz, H.: Gesammelte Werke. Bd. 1. Leipzig (1895)

2. Carrera, E.: Single vs multilayer plate modellings on the basis of Reissner's mixed theorem. AIAA J. **38**(2), 342–352 (2000)
3. Reissner, E.: On a certain mixed variational theory and a proposed applications. Int. J. Numer. Methods Eng. **20**, 1366–1368 (1984)
4. Reissner, E.: On a mixed variational theorem and on a shear deformable plate theory. Int. J. Numer. Methods Eng. **23**, 193–198 (1986)
5. Matsunaga, H.: Vibration and stability of thick plates on elastic foundations. J. Eng. Mech. **1**(27), 27–341 (2000)
6. Kant, T., Swaminathan, K.: Free vibration of isotropic, orthotropic, and multilayer plates based on higher order refined theories. J. Sound Vib. **241**(2), 319–327 (2001)
7. Rao, M., Scherbatiuk, K., Desai, Y., Shah, A.: Natural vibrations of laminated and sandwich plates. J. Eng. Mech. **130**(11), 1268–1278 (2004)
8. Kurpa, L.V., Timochenko, G.N.: Studying the free vibrations of multilayer plates with a complex planform. Int. Appl. Mech. **42**(1), 103–109 (2006)
9. Andrews, G.M., Massabo, R., Cox, B.N.: Elastic interaction of multiple delaminations in plates subject to cylindrical bending. Int. J. Solids Struct. **43**, 855–886 (2006)
10. Zubko, V.I., Shopa, V.M.: Calculation of simply supported circular plates in the statement of the problem of contact interaction in a package of two plates. Mech. Compos. Mater. **43**(5), 409–418 (2007)
11. Zubko, V.I.: Calculation of rigid clamped circular plates in the statement of the problem on contact interaction in a two-layer package. Mech. Compos. Mater. **43**(1), 63–74 (2007)
12. Vangipuram, P., Ganesan, N.: Buckling and vibration of rectangular composite viscoelastic sandwich plates under thermal loads. Compos. Struct. **77**, 419–429 (2007)
13. Pradeep, V., Ganesan, N.: Thermal buckling and vibration behavior of multi-layer rectangular viscoelastic sandwich plates. J. Sound Vib. **310**, 169–183 (2008)
14. Loredo, A., Castel, A.: A multilayer anisotropic plate model with warping functions for the study of vibrations reformulated from Woodcock's work. J. Sound Vib. **332**(1), 102–125 (2013)
15. Altukhov, E.V., Simbratovich, E.V., Fomenko, M.V.: Steady-state vibrations of two-layer plates with rigidly fixed end faces and imperfect contact of the layers. J. Math. Sci. **18**(1), 39–53 (2014)
16. Hoshyarmanesh, S., Bahrami, M.: Molecular dynamic study of pull-in instability of nano-switches. Adv. Nanoparticles **3**, 122–132 (2014)
17. Malekzadeh, K., Mozafari, A., Ghasemi, F.A.: Free vibration response of a multilayer smart hybrid composite plate with embedded SMA wires. Lat. Am. J. Solids Struct. **11**, 279–298 (2014)
18. Akoussan, K., Boudaoud, H., Daya, E.-M., Carrera, E.: Vibration modelling of multilayer composite structures with viscoelastic layers. Mech. Adv. Mater. Struct. **22**, 136–149 (2015)
19. Pietrzakowski, M.: An active functionally graded piezocomposite plate subjected to a stochastic pressure. Arch. Acoust. **40**(1), 101–108 (2015)
20. Bloch, M., Tsukrov, S.Y.: Axisymmetric contact thin cylindrical shells. Calc. Spat. Syst. Constr. Mech. 79–82 (1972) (in Russian)
21. Detinko, F.M., Fastovsky, V.M.: Contact problem of two cylindrical shells of different lengths. Bull. USSR Acad. Sci. Mech. Solids **3**, 118–121 (1974). (in Russian)
22. Detinko, F.M., Fastovsky, V.M.: On the contact on the shroud cylindrical shell. J. Appl. Mech. **11**(2), 124–126 (1975). (in Russian)
23. Bloch, M.B., Tsukrov, S.Y.: The effect of changes in wall thickness on the axisymmetric contact of thin cylindrical shells. J. Appl. Mech. **10**(4), 31–37 (1974). (in Russian)
24. Konveristov, G.B.: Axisymmetric contact problem for a cylindrical shell. Resist. Mater. Thorium Constr. **27**, 119–124 (1975). (in Russian)
25. Konveristov, G.B., Spirina, N.I.: Contact stresses interaction of a cylindrical shell with a bandage. J. Appl. Mech. **15**(2), 65–70 (1979). (in Russian)
26. Pankratova, N.D.: Inhomogeneous deformation of the thick-walled spherical shells at the hard contact layers. Bull. Ukr. Acad. Sci. Ser. A **6**, 49–52 (1984). (in Russian)
27. Stepanov, R.D.: On the bending of the flat rectangular plate, reinforced by parallel ribs or legs. Ing. Sat. 68–79 (1950) (in Russian)
28. Petrushenko, Y.Y.: Variational methods of investigation of strength, stability and dynamic response of spatial structures composed of laminated shells of complex geometry. Appl. Probl. Mech. Shells 76–64 (1989) (in Russian)
29. Drumev, V.K.: Some studies on the stability of circular plates with elastic foundation top. Theor. Appl. Mech. **11**(3), 94–101 (1980)
30. Varvak, P.M., Medvedev, N.M., Perel'muter, A.V., Pinsker, A.G.: Axisymmetric contact problem for several thin shells under finite displacements. Struct. Strength **3**, 35–41 (1978)
31. Vasilenko, A.T., Grigorenko, A.M., Pankratova, N.D.: Problem solving of static thick-walled cylindrical shells with non-rigid contact layers. Bull. Ukr. Acad. Sci. Ser. A **11**, 40–43 (1983). (in Russian)
32. Paimushin, V.N.: The variational methods for solving nonlinear problems of spatial coupling of deformable bodies. Bull. USSR Acad. Sci. **273**, 1083–1086 (1963). (in Russian)
33. Pit'ko, V.V.: Solution of some problems for a spherical shell. Build. Mech. Calc. Struct. **6**, 21–26 (1973)
34. Fomina, N.I.: The problem of determining the lowest natural frequency of the cylindrical shell reinforced by annular transverse and longitudinal rectangular plates. Bull. Ukr. Acad. Sci. Ser. Nat. Techno. Mat. Science **8**(4), 55–59 (1987). (in Russian)
35. Artyukhin, Y.P., Karasev, S.N.: Some contact problems of the theory of thin plates. Issled. Theory Plates Shells **10**, 159–166 (1973)
36. Bloch, M., Tsukrov, S.Y.: On the axisymmetric contact of thin cylindrical shells. Appl. Mech. **9**(11), 23–28 (1973)
37. Pelekh, B.L., Sukhorolsky, M.A.: Contact Problems of the Theory of Elastic Anisotropic Shells. Naukova Dumka, Moscov (1980). (in Russian)
38. Martynenko, YuG: Trends of development of today's gyroscopes. Soros J. Educ. **11**, 120–127 (1997)

39. Awrejcewicz, J., Krysko-jr., V.A., Yakovleva, T.V., Krysko,V.A., Noisy contact interactions of multi-layer mechanical structures coupled by boundary conditions. J. Sound Vib. (2016) (accepted)
40. Sheremetev, A.G.: Fibre optical gyroscope. Radio Connect. **152**, 1–8 (1987)
41. Zhuravlev, V.F., Klimov, D.M.: Wave Hemispherical Gyroscope. Nauka, Moscow (1985)
42. Merkur'ev, V.V., Podalkov, V.V.: Dynamics of Micromechanical and Wave Hemispherical Gyroscope. Fizmatlit, Moscow (2009)
43. Brozgul, I.I., Smirnov, E.L.: Vibrational Gyroscopes. Mashinostroyeniye, Moscow (1970)
44. Li, G., Aluru, R.: Linear, nonlinear and mixed-regime analysis of electrostatic MEMS. Sens. Actuators A Phys. **91**, 278–291 (2001)
45. Buks, E., Roukes, M.L.: Metastability and the casimir effect in micromechanical systems. Europhys. Lett. **54**, 220–226 (2001)
46. Zhang, W., Baskaran, K.L.: Turner effect of cubic nonlinearity on auto-parametrically amplified resonant MEMS mass sensor. Sens. Actuators A Phys. **102**, 139–150 (2002)
47. Kantor, B.J.: Nonlinear Problems of the Theory of Inhomogeneous Shallow Shells. Science. Dumka, Kiev (1971). (in Russian)
48. Kantor, B.J.: Contact Problems of the Nonlinear Theory of Shells. Science. Dumka, Kiev (1990). (in Russian)
49. Kirichenko, V.A., Krysko, V.A.: Substantiation of the variational iteration method in the theory of plates. Sov. Appl. Mech. **17**(4), 366–370 (1981)
50. Birger, I.A., Mavlyutov, R.R.: The Resistance of Materials. Nauka, Moscow (1986). (in Russian)
51. Ladyzenskaja, O.A., Ural'ceva, N.N.: Linear and Quasilinear Elliptic Equations. Academic, New York (1968)